Space Weather

RESEARCH ARTICLE
10.1029/2024SW004238

Key Points:

- Inner zone proton flux increase over four solar cycles passes maximum
- NOAA-15, NOAA-19 and modeled proton flux all show anti-correlation with changes in F10.7 as proxy for EUV
- Long-term behavior of protons suggests Centennial Gleissberg Cycle in solar activity has passed minimum

Correspondence to:

K. Adams,
Kalvyn.Adams@colorado.edu

Citation:

Adams, K., Bregou, E., Hudson, M., Kress, B., & Selesnick, R. (2025). Turnover in Gleissberg Cycle dependence of inner zone proton flux. *Space Weather*, *23*, e2024SW004238. https://doi.org/10.1029/2024SW004238

Received 2 NOV 2024
Accepted 26 JAN 2025

Author Contributions:

Conceptualization: Mary Hudson
Data curation: Kalvyn Adams, Emily Bregou, Mary Hudson, Richard Selesnick
Formal analysis: Kalvyn Adams, Mary Hudson
Funding acquisition: Mary Hudson
Investigation: Kalvyn Adams, Mary Hudson
Methodology: Emily Bregou, Mary Hudson
Project administration: Mary Hudson
Resources: Mary Hudson, Brian Kress
Software: Kalvyn Adams, Emily Bregou
Supervision: Mary Hudson, Brian Kress, Richard Selesnick
Validation: Mary Hudson, Brian Kress, Richard Selesnick
Visualization: Kalvyn Adams, Emily Bregou
Writing – original draft: Kalvyn Adams
Writing – review & editing: Kalvyn Adams, Emily Bregou, Mary Hudson, Brian Kress

Turnover in Gleissberg Cycle Dependence of Inner Zone Proton Flux

Kalvyn Adams[1,2], Emily Bregou[3,4], Mary Hudson[2,4], Brian Kress[5], and Richard Selesnick[6]

[1]Department of Astrophysical and Planetary Sciences, University of Colorado, Boulder, CO, USA, [2]Physics and Astronomy Department, Dartmouth College, Hanover, NH, USA, [3]Department of Physics and Astronomy, University of Pennsylvania, Philadelphia, PA, USA, [4]NCAR High Altitude Observatory, Boulder, CO, USA, [5]Center for Cooperative Research in the Environmental Sciences at CU Boulder, Boulder, CO, USA, [6]Space Vehicles Directorate, Air Force Research Laboratory, Kirtland AFB, NM, USA

Abstract The NOAA POES satellites orbit through the South Atlantic Anomaly (SAA) allowing access to the trapped inner belt high energy proton population. A previous study found a long-term increase in proton flux averaged over the 11-year solar cycle oscillation corresponding to solar activity consistent with the Centennial Gleissberg Cycle (CGC). F10.7 flux maxima have been decreasing over the ∼40-year period of 1980–2021, correlating with an average increase in the varying proton population. Bregou et al. ’s (2022, https://doi.org/10.1029/2022sw003072) long-term study of the peak flux over the SAA in NOAA-15 shows an increase in proton flux from 1998 until 2021. The observed flux increase is correlated with both the ∼11-year solar cycle and the overall decreasing F10.7 flux over the period studied. This long-term decrease in F10.7 flux and increase in proton flux is concluded to be the manifestation of the CGC minimum and accompanying decrease in solar Extreme Ultraviolet irradiance (EUV). We extend Bregou et al., ’s (2022, https://doi.org/10.1029/2022sw003072) study to 2024 and observe a rapid increase in F10.7 flux at the beginning of Solar Cycle 25, a proxy for EUV, leading to increased proton loss to the expanding atmosphere and a steep decrease in the inner zone proton flux from 2022 to 2024 in NOAA-15 and NOAA-19 measurements. A model calculation of the inner zone proton flux generally agrees with the long-term trend in flux magnitude.

Plain Language Summary The Earth's inner radiation belt, dominated by high-energy protons, is influenced by solar activity. Studies have shown a correlation between the 11-year solar cycle and the proton population, with lower solar activity leading to increased proton flux. We analyzed data from NOAA-15 and NOAA-19 satellites to monitor the proton population above the South Atlantic Anomaly. Our findings indicate that the recent increase in solar activity, causing a significant decline in the proton flux, is correlated with the turnover in the Centennial Gleissberg Cycle, a longer-term modulation of solar activity spanning approximately 80–100 years. As solar activity continues to rise over the next few solar cycles, we anticipate a further decrease in the proton population. This changing space climate will have implications for the design and operation of future satellite missions.

1. Introduction

The space weather surrounding Earth strongly affects the inner and outer Van Allen radiation belts, also referred to as the inner and outer zone, responding to solar activity which causes spacecraft anomalies and disruptions of technological systems on which society depends (Baker, 2000). The inner belt specifically is formed with a population of 10–1,000 MeV protons and electrons in the keV range trapped by the Earth's magnetic field at $\sim 10^3$ km (Schulz & Lanzerotti, 1974). Cosmic Ray Albedo Neutron Decay (CRAND) serves as the primary source for high energy protons at low altitude while Solar Energetic Proton trapping dominates at the outer edge of the inner zone at lower energies (Selesnick et al., 2007). High energy protons that populate the inner zone can be damaging to low altitude satellites that pass-through the South Atlantic Anomaly (SAA), where the Earth's magnetic field is weakest and trapped fluxes are most intense (Dyer, 2002; Stassinopoulos & Raymond, 1988). Predicting trends in the population of trapped protons has a key importance in planning satellite missions and the anti-correlation between solar activity and proton flux in the inner radiation belt has been well studied (Bregou et al., 2022; Bruno et al., 2021; Dragt, 1971; Huston et al., 1998; Kuznetsov et al., 2010; X. Li et al., 2020; Lin et al., 2020; Nakano & Heckman, 1968; Qin et al., 2014). As solar activity, that is, sunspots, solar flares, and coronal mass ejections, increase, solar Extreme Ultraviolet irradiance (EUV), photoionization, and auroral

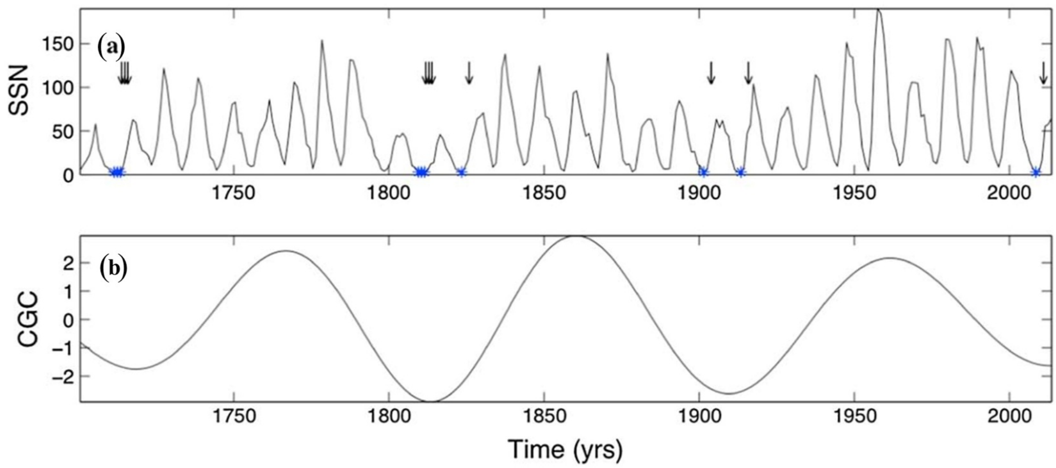

Figure 1. From Feynman and Ruzmaikin (2014), (a) shows the annual sunspot number record from 1700 to 2012. Each arrow and asterisk included in panel (a) specifies a time when the annual sunspot number was less than 3. Panel (b) shows the time series of the 80–110-year Centennial Gleissberg Cycle in sunspot number on a log scale.

activity also increase (Gombosi, 1998). The increase in EUV irradiance heats up and expands the atmosphere, causing an increase in neutral particle collisions at higher altitudes. Photoionization and auroral electron precipitation also contribute to the increase in the ionospheric scale height (Gombosi, 1998). Coulomb collisions with free and bound electrons serve as the primary loss mechanism for inner zone protons (Selesnick et al., 2007). This connection to solar activity creates a pattern anti-correlated with the solar cycle as a long-term trend, as found by Qin et al. (2014), X. Li et al. (2020), and Bregou et al. (2022).

The solar cycle is largely characterized by the approximately 11-year cycle between sunspot minima or maxima. However, studying long-term records, Gleissberg (1939) found a periodic fluctuation of sunspot numbers that recurs every seven to eight solar cycles. The Centennial Gleissberg Cycle (CGC) has also been established through ice core records and auroral records (Feynman & Ruzmaikin, 2014). Feynman and Ruzmaikin's (2014; Figure 1), reproduced below, shows the solar cycle variation all the way up to 2012 including the predicted solar cycle 23–24 extended solar minimum, indicating a CGC minimum.

Feynman and Ruzmaikin (2014) also noted that "Solar Cycles 23 and 24 exhibited an extended, deep minimum," in line with the expected approach of the CGC minimum. This long-term solar activity trend, coupled with the anticorrelation between solar activity and proton flux, has been reported in the long-term increase of inner zone proton flux over the previous four solar cycles (Bregou et al., 2022).

Bregou et al. (2022) studied the inner zone proton flux and its anticorrelation with solar cycle activity using the NOAA Polar Orbiting Environmental Satellite fleet (POES). This low altitude weather satellite fleet includes NOAA-06–NOAA-19 and MetOp satellites supported by the UK-EU carrying the same instrumentation as on NOAA-15–19 (https://www.ncei.noaa.gov/products/poes-space-environment-monitor). All are in sun-synchronous orbits between 800 and 870 km above the surface of the Earth. The primary satellites used in the Bregou et al. (2022) study include the NOAA-12 and 15 satellites, and their study incorporated data from Qin et al. (2014) using NOAA-06, 10, and 12 measurements. In this study we incorporate data from the NOAA-15 and NOAA-19 satellites. These satellites carried the upgraded Space Environment Monitor SEM-2. The SEM-1 included the Medium Energy Proton and Electron Detector (MEPED) with omnidirectional energy channels 16–215, 36–215, and 80–215 MeV. The SEM-2 carried the MEPED with energy channels >16, >35, >70, and >140 MeV (Evans & Greer, 2006). The POES (and MetOp) satellites pass over the SAA, an area where Earth's magnetic field is weaker due to the offset between Earth's geometric center and magnetic dipole center and higher order multipole components (Pavón-Carrasco & De Santis, 2016), that allows for high energy protons trapped in Earth's inner-radiation belt to be observed at lower altitudes before mirroring, as they bounce between northern and southern hemispheres.

Bregou et al. (2022) showed data up until June 2021, approaching the inner zone proton flux maximum following the 2019 minimum between Solar Cycles 24 and 25. This paper extends their study of the trapped proton

Table 1
The Longitudinal Ranges Used for the South Atlantic Anomaly for Each NOAA Spacecraft Over Time, Updated From Qin et al. (2014)

Spacecraft	Longitude range (°)
NOAA-06	[−48, −42]
NOAA-10	[−50, −44]
NOAA-12	[−52, −46]
NOAA-15 (1998–2009)	[−53, −47]
NOAA-15 (2009–2024)	[−55, −49]
NOAA-19 (2009–2024)	[−55, −49]

population by 3 years using NOAA-15 and the higher altitude NOAA-19. In the extended POES data figures to follow, there is a decrease seen with the inclusion of data through September 2024. A model calculation of the inner zone proton flux using F10.7 based on (Selesnick et al., 2007) is also compared to the NOAA-15 measurements, validating the overall structure of the long-term trend. With measurements of F10.7 in Solar Cycle 25 already higher than Solar Cycle 24 (https://www.swpc.noaa.gov/products/solar-cycle-progression), we expect to see the next minimum in the protons to be lower than the minimum caused by the previous solar maximum and resulting forcing of an expanded atmosphere and increased collisional loss. This matches predictions that the CGC minimum passed between Solar Cycle 24 and 25, and we should expect a solar-cycle averaged decrease in the inner zone proton population with increasing solar activity over the next ∼40 years.

The paper is structured as follows. In Section 2, Methods, we discuss the long-term data analysis of the POES satellite data. In Section 3, Observational Results, we examine Figure 1 from Bregou et al. (2022) showing the long-term trend in the proton flux. We then extend their study through September 2024 in the >70 MeV channel of NOAA-15. The same method is applied to the NOAA-19 data to validate that the same trend is seen at different altitudes and determine how it varies with altitude. In Section 4 a phase lag calculation is performed between F10.7 and proton flux data between 2009 and 2024, to capture the most recent delay between solar minimum and proton flux maximum. In Section 5 the NOAA-15 data is compared to a model calculation of the inner zone proton population from Selesnick et al. (2007) and found to be consistent with the satellite findings. Lastly, the Discussion and Conclusions covers the implications of the recent measurements (which are averaged over a 3-month interval as described below) for the long-term variation of inner zone proton flux with implications for further study of the Gleissberg Cycle.

2. Methods

To focus on the long-term evolution of the inner zone proton flux, we implement temporal averaging and exclude periods of Solar Energetic Protons (SEP) associated with solar flares, coronal mass ejections and geomagnetic storms which give protons temporary access to lower latitudes and the polar regions (Z. Li et al., 2021). The proton population is only visible to the NOAA satellites above the poles (un-trapped on open magnetic field lines) and above the SAA, where the trapped population extends to lower altitudes due to the Earth's weaker magnetic field in this region. To account for these effects and to mitigate the day-to-day variance of the proton flux, Bregou et al. (2022) defined a set of conditions for data to be used from NOAA-15. We extended these conditions for NOAA-15 into 2024 and propagated the conditions over the data from the NOAA-19 satellite to corroborate the results from NOAA-15 and to examine altitude dependence.

The first condition imposed is the exclusion of data on days when the satellite is detecting counts above 20 in the 140 MeV range while above the Earth's poles (>60 latitude, <−60 latitude) since such measurements are an indicator of short-lived, un-trapped SEP flux. The second condition is that the only data considered falls within the boundary of the SAA defined by Qin et al. (2014). The latitudinal range sits consistently between −60° and 20°. The longitudinal range defined by Qin et al. (2014) over time, as the SAA shifts due to very long-term changes in the Earth's magnetic field, is shown below in Table 1.

The final piece is finding the maximum flux in the SAA over a 3-month (specifically 90 day) period to further reduce short-term variability in the data. Following Qin et al. (2014) and Bregou et al. (2022), we fit a Gaussian in latitude over the adjusted proton flux data. As shown by Qin et al., 's (2014) study, fitting a Gaussian to the proton flux in longitude or latitude results in correlation coefficients close to 1, suggesting either fit as a suitable description of the distribution of the SAA and that both fit results are close to the measured value. Using the fitted Gaussian over the 90 days, we take the estimated peak flux value over the latitudinal distribution as the resulting data point for the 3-month period. A change between the method used by Bregou et al. (2022) and that implemented here is made where the 90-day period resets. Instead of resetting the 90-day count at the beginning of each calendar year, we allow the 90-day count to continue through the end of 1 year and into the next year to maintain a fixed number of days in each sampling interval. This change causes only minor differences in counts between the two studies.

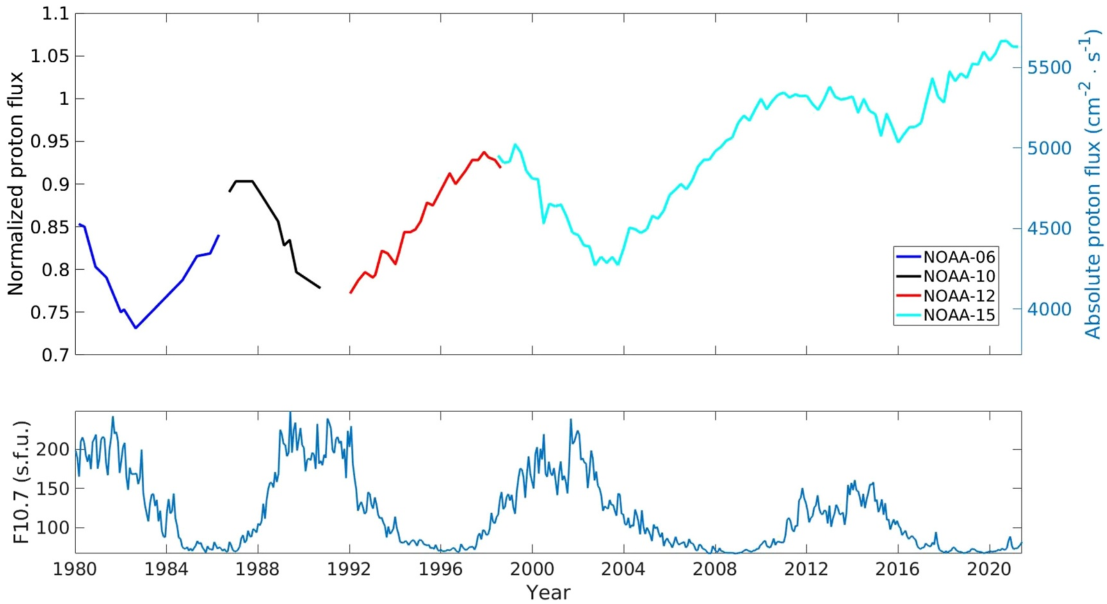

Figure 2. Three-month averaged peak flux for >70 MeV protons in the South Atlantic Anomaly is normalized to flux (=1) at the beginning of 2010 (top) and plotted against 10.7 cm solar flux (F10.7, bottom) from 1980 to June 2021 to extend Figure 3 in Qin et al. (2014) which covered 1980 through 2009. Different colors are used to represent different POES satellites. Prior to the NOAA-15 data beginning in 1999, satellites measured >80 MeV proton flux. Qin et al. (2014) found good agreement between the >80 MeV and >70 MeV proton flux data and determined that no correction factor was necessary. (F10.7 flux in s.f.u. = 10^{-22} W m^{-2} Hz^{-1}) (Source: Bregou et al., 2022).

3. Observational Results

With the preceding constraints on POES data included in our study, we next converted from counts to flux as described by Bregou et al. (2022), using the appropriate geometric factor for the MEPED instrument. Examining Figure 2, we can see a maximum in proton flux in 2022 consistent with the solar cycle oscillation in F10.7 seen in previous solar cycles. We use F10.7 here as a proxy for EUV irradiance coming from the Sun. In the following figures we extend the NOAA-15 (and NOAA-19) >70 MeV proton data through September 2024, wherein the flux is seen to drop rapidly and below the previous proton flux minimum in the NOAA-19 data, correlated with the faster increase in F10.7 seen early in Solar Cycle 25 when compared with Solar Cycle 24. As noted by Lugaz et al. (2023), sunspot number (and F10.7) is now as high as it has been for over 20 years.

Figure 3 compares >70 MeV proton flux measured by NOAA-15 and NOAA-19 from 1999 to 2024 with F10.7. The maximum proton flux is seen in 2022 followed by a downward trend continuing through September 2024. The comparison with NOAA-19 proton flux at >70 MeV begins in October of 2013 following launch, when the raw netCDF data from the Space Environment Monitor became available (https://www.ncei.noaa.gov/products/poes-space-environment-monitor, raw level 1a Data), with corresponding measurements from NOAA-15. NOAA-19 was at a higher altitude (870 vs. 820 km apogee) and thus measured higher proton flux on the steeply rising inner gradient of the proton inner zone (Selesnick & Albert, 2019). Both see the 2022 proton flux maximum fall steeply in 2024, as F10.7 reaches values last seen at the Solar Cycle 23 maximum ~2000. It is also seen in the NOAA-19 data that the proton flux drops below the level of the previous flux minimum in 2016 indicated with straight lines.

During September and October of 2024, the proton flux began to drop below the previous minimum in 2016 in NOAA-19 data, which is consistent with the turnover in the CGC, as manifest in the average inner zone proton flux. The small amplitude periodic variation (~120-day periodicity) also apparent in Figure 2 is due to the precession of the orbit, with the peaks corresponding to apogee in the Southern Hemisphere and above the SAA and the dips corresponding to perigee in the Southern Hemisphere, where the flux is lower on the inner edge of the proton inner zone at lower altitudes. See Selesnick and Albert (2019) for radial profiles of the proton inner zone from Van Allen Probes spacecraft measurements inside L = 5.8 (radial distance in Earth radii) in the near equatorial plane from October 2013 to January 2019, with steeply falling flux between L = 1.2–1.4. The region of

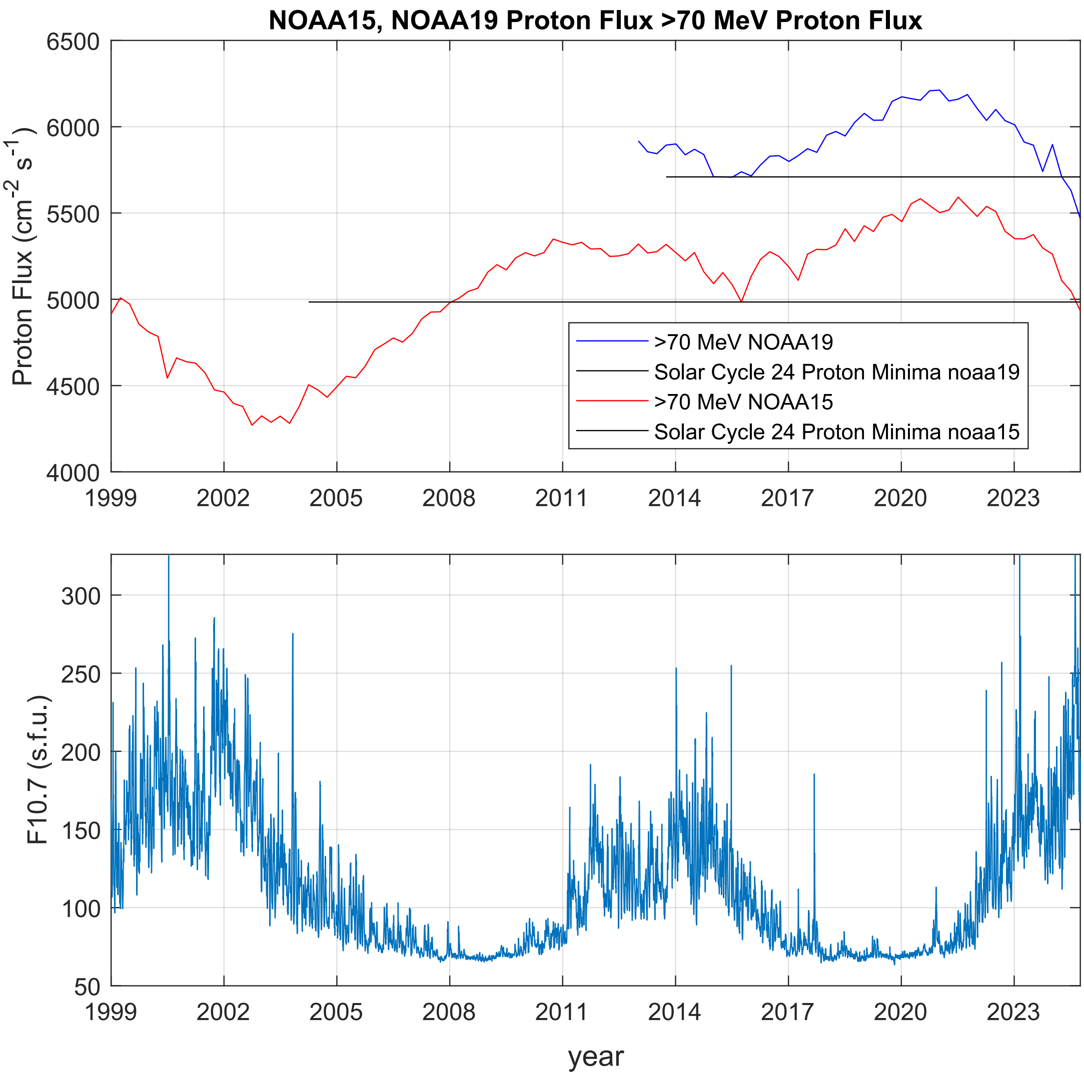

Figure 3. (top) Similar criterion applied to the NOAA-15 data (red) is applied to the NOAA-19 data (blue) corroborating the turnover point in the NOAA-15 data. The 2016 proton flux minimum is indicated with a black line for both satellites. (bottom) F10.7 cm data as a proxy for solar activity for comparison.

maximum flux at POES altitude in the SAA is close to L = 1.3 (Figure 2, Bregou et al., 2022, see also their Figure S2).

The MEPED on the SEM instrument (an instrument on both NOAA-15 and NOAA-19) includes proton energy channels for >16, >35, >70, >140 MeV. We next use the same method of data selection for >70 MeV with the >35 and >140 MeV channels, excluding the >16 MeV channel which is subject to electron contamination (Janet Green, private communication), showing that the trend in the protons transcends energy levels and is not specific to just the >70 MeV energy range. Figure 4 includes the long-term study of the three energy channels from NOAA-15 with the extension into 2024.

4. Proton Flux Maximum Lag Following Solar Minimum

Bregou et al. (2022) obtained an ∼500-day lag period between the inflection points of solar activity and proton flux for the period 1 January 2010–1 June 2021 due to the time scale of proton energy loss at the altitude of the NOAA satellites (Selesnick et al., 2007). The EUV's effect on inner zone proton loss dominates over the solar cycle modulation in Galactic Cosmic Rays and subsequently the CRAND source for inner zone proton flux as shown by X. Li et al. (2020), who compared the ∼4% solar cycle variation in ground-based neutron monitor flux

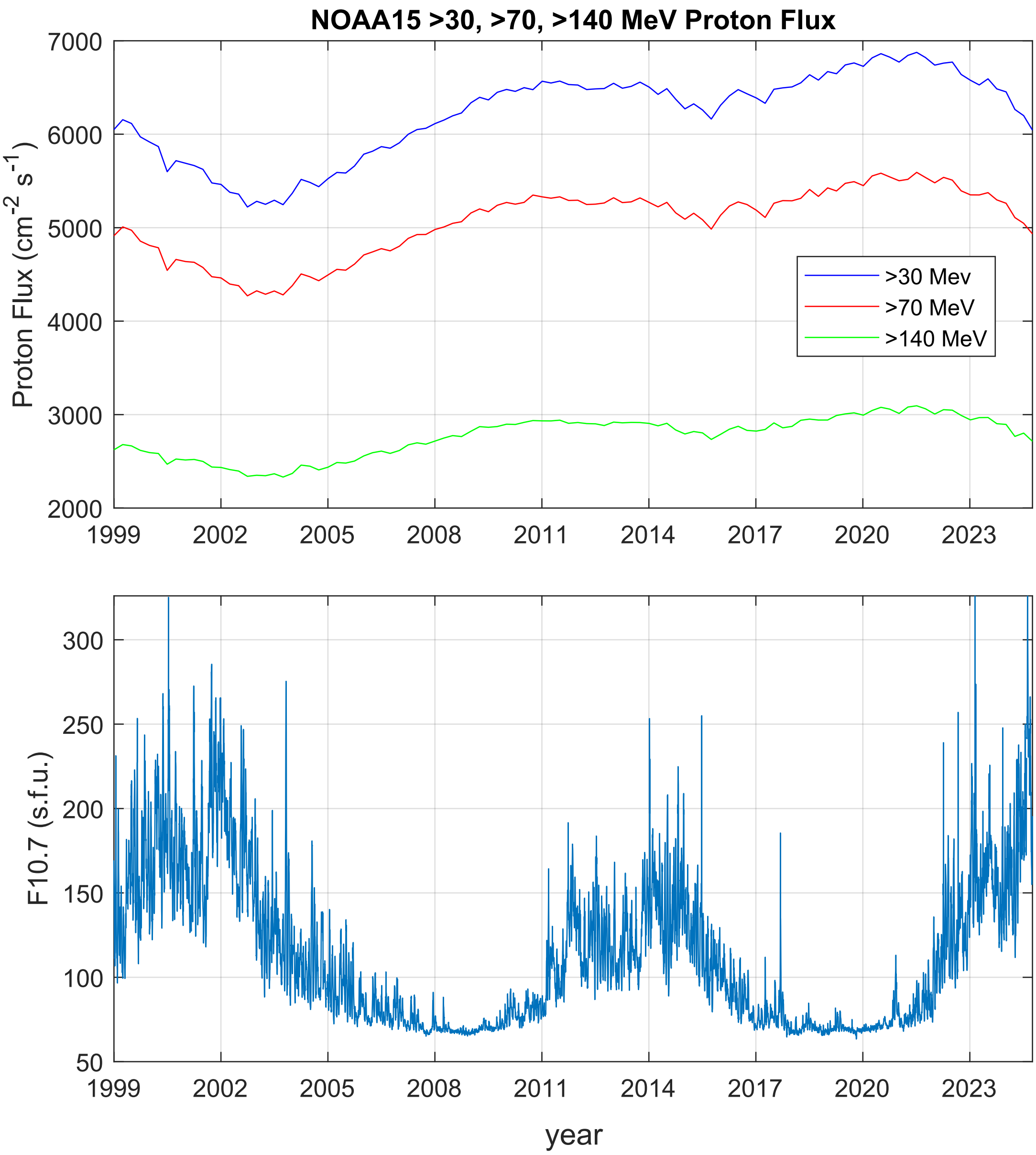

Figure 4. (top) Similar criteria applied to the >70 MeV data (red) applied to the >35 MeV data (blue) and >140 MeV data (green) showing the same trend across energy levels. Thresholds for the 2016 proton flux minimum for all three energy channels are provided in black. (bottom) F10.7 cm data as a proxy for solar activity for comparison.

(indicating Galactic Cosmic Rays) (Delaware, L = 2.4) with measured 300% variation in proton flux by the SAMPEX satellite (Baker et al., 2012). The maximum in proton flux ~500 days after the end of 2019 is consistent with the passing of the most recent solar cycle minimum between Solar Cycle 24 and 25. This would suggest a peak in proton flux around the middle of 2021, and the turnover point to be visible in data from 2021 to 2024 in our extended study. We recreate the lag time calculation with the data extended into 2024, producing a similar lag time of ~550–650 days in Figure 5.

In Figure 5, a correlation coefficient is calculated between a 15-year selection of the proton flux and F10.7 (starting 2009–2024). The time selection of the F10.7 is then moved backwards in time by a 5-day timestep, and the correlation coefficient is calculated again, up to 800 days. This same correlation coefficient is repeated for all three energy channels. This correlation coefficient matches the anti-correlation previously reported between the proton flux and F10.7, greatest between 550 and 650 days averaged between all three channels. This lag time

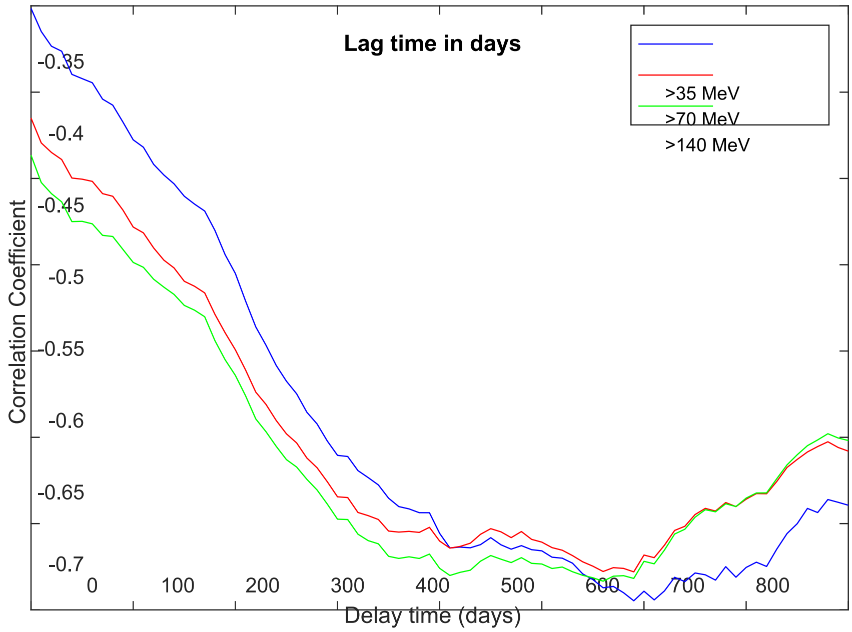

Figure 5. Correlation coefficient calculated between selections of time in the proton flux and the F10.7 with the time selection of F10.7 behind the proton flux by an increasing number of days (to show the lag). This calculation is repeated for all three energy channels.

which is consistent with the observed flux maximum in 2022 also falls within the range determined by Qin et al. (2014) of 380–705 days for the period 1 January 1980–31 December 2009, seen in Figure 2.

5. Model Comparison

Alongside the data from NOAA-15 presented in Bregou et al. (2022), they have compared the results from a theoretical model of the inner zone protons (Selesnick et al., 2007), as updated by Selesnick and Albert (2019). The model includes the CRAND proton source, atmospheric and plasmaspheric drag causing proton energy loss, a stochastic implementation of radial diffusion, and a model geomagnetic field (IGRF) including secular variation. Models of the atmosphere, plasmasphere, and Galactic Cosmic Ray spectra are each parameterized by F10.7 and are used to compute the variable CRAND source and energy loss rates based on proton drift-shell averaging as a function of the three adiabatic invariants of trapped particle motion. Model results showing the maximum omnidirectional integral (>70 MeV) proton flux in the SAA region at NOAA-15 altitude, as a function of time from 1980 to 2021, are shown in Figure 6, for comparison with the NOAA-15 observations in Figure 3. The trend of generally increasing proton flux up until June 2021, with a superimposed solar-cycle modulation, as seen in the proton flux measurements, is also evident in the model results. We make the same comparison as Bregou et al. (2022), using a 1.13 numerical factor to reduce the simulated flux, and show that the shape of the model and the satellite measurements (updated with an exact 90-day flux Gaussian to the fit peak flux as described in Section 2) for >70 MeV protons are in agreement up to the flux maximum.

6. Discussion and Conclusions

Following the predictions of the CGC (Feynman & Ruzmaikin, 2014; Gleissberg, 1939; Svalgaard et al., 2005; Upton & Hathaway, 2018), updated with more recent NOAA POES measurements of inner zone proton flux and F10.7, and extended 3 years beyond the study of Bregou et al. (2022), an observed flux turnover is seen in Figures 3 and 4. These observations project an average decrease in inner zone proton flux following the Solar Cycle 25 maximum relative to that following the Solar Cycle 24 maximum. This decrease is due to increased collisional energy loss of protons as the atmosphere expands with increased solar activity. Both the NOAA-15 and NOAA-19 measurements show the turnover following the proton flux maximum. This confirms the well-known solar cycle modulation of inner zone proton flux, while the precipitous drop in flux in 2024 seen in Figure 3,

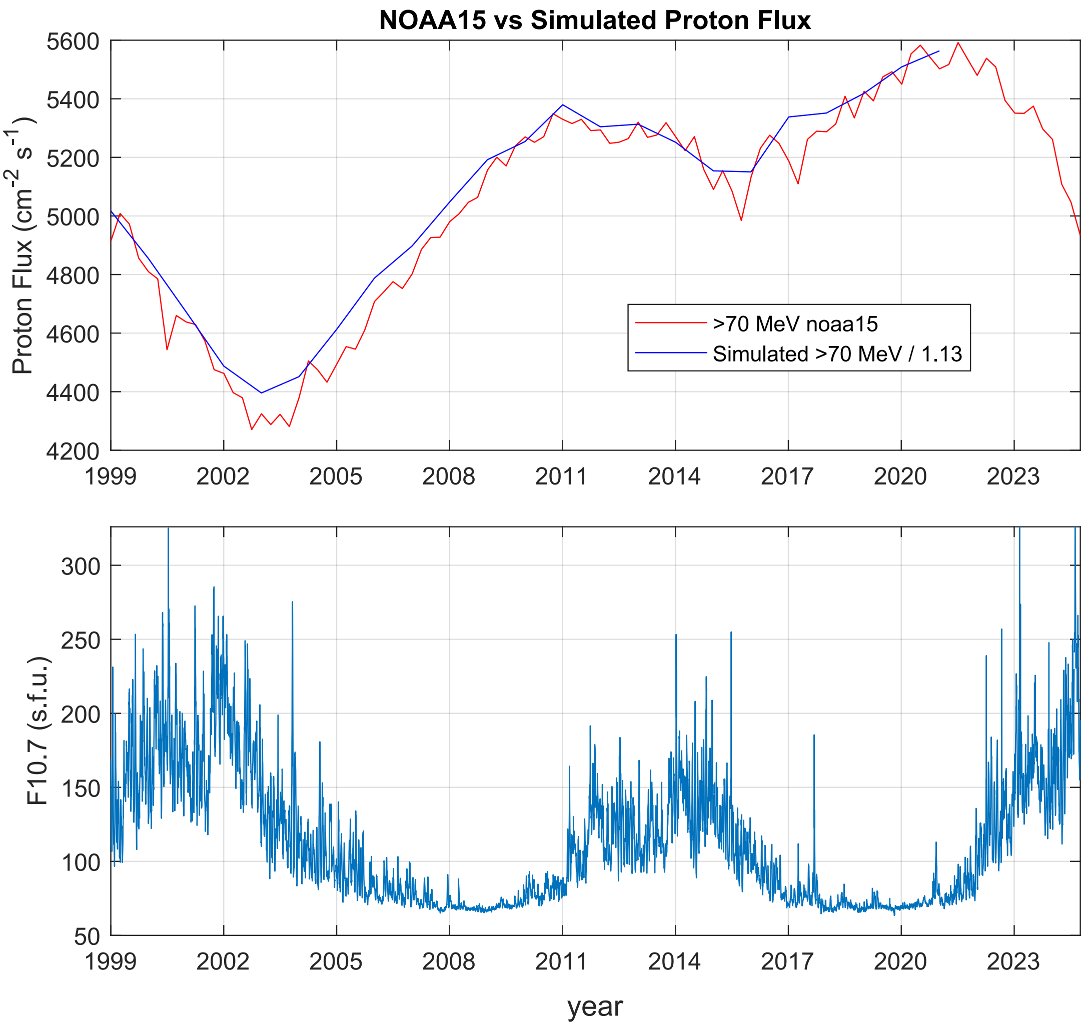

Figure 6. (top) In red, the 3-month block averaged method applied to NOAA-15's data. In blue, the yearlong proton flux counts from Selesnick's model of the inner zone radiation belt (Selesnick & Albert, 2019; Selesnick et al., 2007) using the same selection process. A numerical factor of 1.13 is removed from Selesnick's model to align the shapes of the graphs. (bottom): F10.7 data directly showing solar activity.

dropping below the last minimum flux level in the NOAA 19 data, occurs ahead of the NOAA solar maximum forecast shown in Figure 7, suggesting that the Centennial Gleissberg minimum and associated flux maximum recognized by Bregou et al. (2022) has passed. Neutral density increases with F10.7 at the altitude of both NOAA-15 and NOAA-19 for molecular and heavier (than hydrogen) atomic species, with a faster relative increase at higher altitudes (Selesnick et al., 2007, Figure 11, based on NRLMSISE-00; Yue & Wang, 2024). This thermospheric density dependence on altitude and F10.7 suggests that the faster decrease in proton flux seen by NOAA-19 (870 km apogee) relative to NOAA-15 (820 km apogee), when compared with the minimum flux for Solar Cycle 24 indicated by the black lines in Figure 3, is explained by the difference in thermospheric density at the two altitudes determining the proton energy loss rate (Selesnick et al., 2007). A polynomial fit to the NOAA-15 (820 km apogee) data in Figure 3 (not shown) projects that the NOAA-15 flux will drop below the 2016 flux minimum following Solar Cycle 24, indicated by the bottom black line in Figure 3, by 31 December 2024.

Other signs of the CGC minimum passing and an increase in solar activity can be found in sunspot number and maximum predictions in McIntosh et al. (2023) and Upton and Hathaway (2023) indicating values higher than Solar Cycle 24's. Increased solar activity, the superstorm of May 2024 as a prime example (https://www.swpc.noaa.gov/news/historical-comparison-may-2024-solar-storms), will lead to decreased proton flux in the inner radiation belt at low altitudes over the SAA, thereby decreasing the risk of damage in low earth orbit which can be

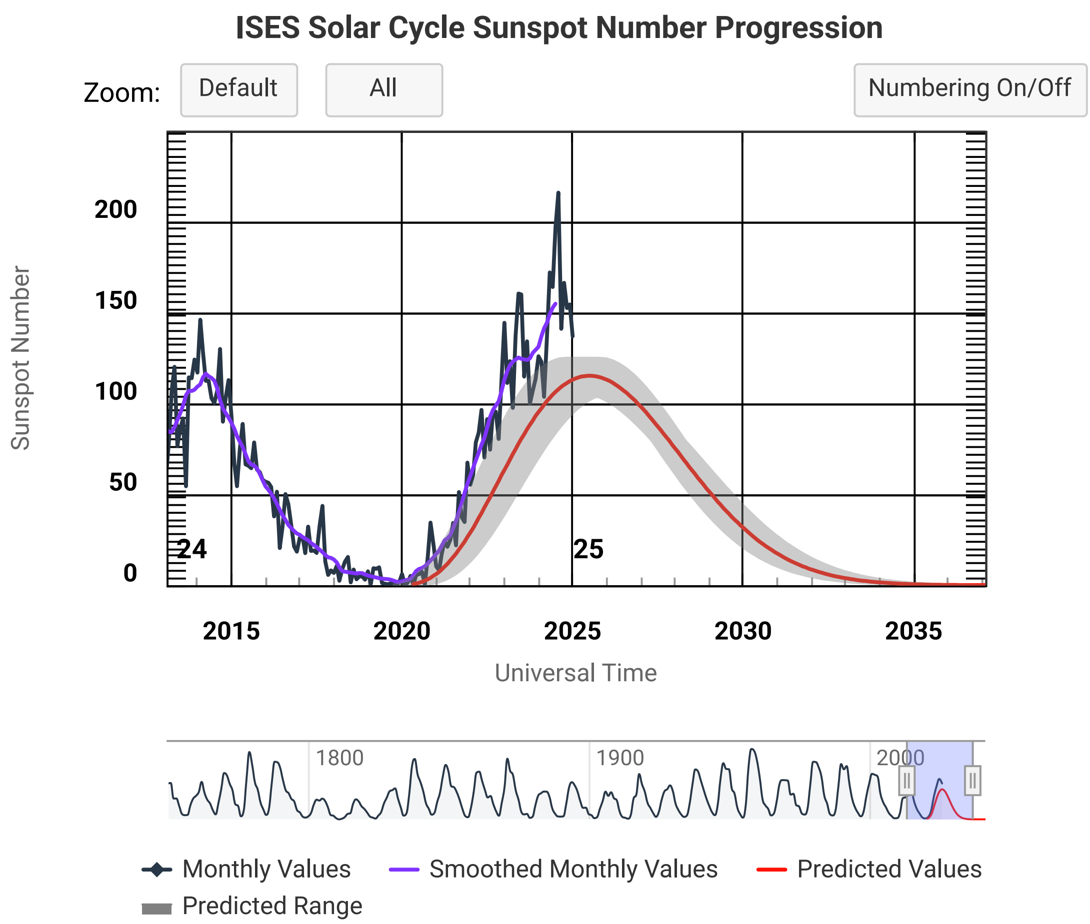

Figure 7. NOAA's International Space Environment Services Solar Cycle Sunspot Number and Model predictions as of July 2024. The figure shows the predicted sunspot number (red) and predicted range (gray) underpredicting severely the observed monthly sunspot number (black) and smoothed monthly values (blue). This forecast is now updated monthly at the NOAA Space Weather Prediction Testbed: https://testbed.swpc.noaa.gov/products/solar-cycle-progression-updated-prediction-experimental.

attributed to the very energetic inner zone protons. This includes damage to solar panels as well as single event upsets in electronics (Dyer, 2002; Horne et al., 2013; Stassinopoulos & Raymond, 1988). As LEO and Medium Earth Orbit (MEO) becomes increasingly populated with spacecraft for communications and navigation, the design and management of satellite systems require taking less well-known long-term variations such as the Centennial Gleisberg Cycle into account, in planning future spacecraft missions, as discussed for example, in: Planning The Future Space Weather Operations and Research Infrastructure Workshop from the National Academies of Sciences, Engineering, and Medicine (2021, 2022).

Data Availability Statement

F10.7 data come from the OMNI database: https://omniweb.gsfc.nasa.gov/form/dx1.html. The data for POES are available at https://www.ncei.noaa.gov/products/poes-space-environment-monitor.

Acknowledgments
Dartmouth College and University of Colorado acknowledge support from AFOSR Grants FA9550-20-1-0339 and FA9550-23-1-0629. The authors acknowledge computing support from NCAR CISL. We thank Ms. Audrey Robison of UNH for helpful discussions. K.A. thanks staff at the NCAR High Altitude Observatory for their gracious hospitality to summer students.

References

Baker, D. N. (2000). The occurrence of operational anomalies in spacecraft and their relationship to space weather. *IEEE Transactions on Plasma Science*, *28*(6), 2007–2016. https://doi.org/10.1109/27.902228

Baker, D. N., Mason, G. M., & Mazur, J. E. (2012). SAMPEX to reenter atmosphere: Twenty-year mission will end. *Space Weather*, *10*(5). Portico. https://doi.org/10.1029/2012sw000804

Bregou, E. J., Hudson, M. K., Kress, B. T., Qin, M., & Selesnick, R. S. (2022). Gleissberg cycle dependence of inner zone proton flux. *Space Weather*, *20*(7), e2022SW003072. https://doi.org/10.1029/2022SW003072

Bruno, A., Martucci, M., Cafagna, F. S., Sparvoli, R., Adriani, O., Barbarino, G. C., et al. (2021). Solar-cycle variations of South Atlantic anomaly proton intensities measured with the PAMELA mission. *The Astrophysical Journal Letters*, *917*(2), L21. https://doi.org/10.3847/2041-8213/ac1a74

Dragt, A. J. (1971). Solar cycle modulation of the radiation belt proton flux. *Journal of Geophysical Research*, *76*(10), 2313–2344. https://doi.org/10.1029/JA076i010p02313

Dyer, C. (2002). Radiation effects on spacecraft & aircraft. In *Solspa 2001, Proceedings of the Second Solar Cycle and Space Weather Euroconference* (Vol. 477, pp. 505–512).

Evans, D. S., & Greer, M. S. (2006). Polar Orbiting Environmental Satellite Space Environment Monitor—2 Instrument Descriptions and Archive Data Documentation.

Feynman, J., & Ruzmaikin, A. (2014). The Centennial Gleissberg Cycle and its association with extended minima. *Journal of Geophysical Research: Space Physics*, *119*(8), 6027–6041. https://doi.org/10.1002/2013JA019478

Gleissberg, W. (1939). A long-periodic fluctuation of the sun-spot numbers. *The Observatory*, *62*, 158–159.

Gombosi, T. I. (1998). *Physics of the Space Environment*. Cambridge University Press. https://doi.org/10.1017/CBO9780511529474

Horne, R. B., Glauert, S. A., Meredith, N. P., Boscher, D., Maget, V., Heynderickx, D., & Pitchford, D. (2013). Space weather impacts on satellites and forecasting the Earth's electron radiation belts with SPACECAST. *Space Weather*, *11*(4), 169–186. https://doi.org/10.1002/swe.20023

Huston, S. L., Kuck, G. A., & Pfitzer, K. A. (1998). Solar cycle variation of the low-altitude trapped proton flux. *Advances in Space Research*, *21*(12), 1625–1634. https://doi.org/10.1016/S0273-1177(98)00005-2

Kuznetsov, N. V., Nikolaeva, N. I., & Panasyuk, M. I. (2010). Variation of the trapped proton flux in the inner radiation belt of the Earth as a function of solar activity. *Cosmic Research*, *48*(1), 80–85. https://doi.org/10.1134/S0010952510010065

Li, X., Xiang, Z., Zhang, K., Khoo, L., Zhao, H., Baker, D. N., & Temerin, M. A. (2020). New insights from long-term measurements of inner belt protons (10s of MeV) by SAMPEX, POES, Van Allen Probes, and simulation results. *Journal of Geophysical Research: Space Physics*, *125*(8), e2020JA028198. https://doi.org/10.1029/2020JA028198

Li, Z., Engel, M., Hudson, M., Kress, B., Patel, M., Qin, M., & Selesnick, R. (2021). Solar energetic proton access to the inner magnetosphere during the September 7–8, 2017 event. *Journal of Geophysical Research: Space Physics*, *126*(7), e2021JA029107. https://doi.org/10.1029/2021JA029107

Lin, R., Zhang, J., Zhang, X., Ni, B., Liu, S., Shi, L., et al. (2020). Long-term variations of >16-MeV proton fluxes: Measurements from NOAA POES and EUMETSAT MetOp satellites. *Journal of Geophysical Research: Space Physics*, *125*(9), e2019JA027635. https://doi.org/10.1029/2019JA027635

Lugaz, N., Liu, H., Carter, B. A., Gannon, J., Zou, S., & Morley, S. K. (2023). New space companies meet a "normal" solar maximum. *Space Weather*, *21*(9), e2023SW003702. https://doi.org/10.1029/2023SW003702

McIntosh, S. W., Leamon, R. J., & Egeland, R. (2023). Deciphering solar magnetic activity: The (solar) hale cycle terminator of 2021. *Frontiers in Astronomy and Space Sciences*, *10*, 1050523. https://doi.org/10.3389/fspas.2023.1050523

Nakano, G. H., & Heckman, H. H. (1968). Evidence for solar-cycle changes in the inner-belt protons. *Physical Review Letters*, *20*(15), 806–809. https://doi.org/10.1103/PhysRevLett.20.806

National Academies of Sciences, Engineering, and Medicine. (2021). *Planning the Future Space Weather Operations and Research Infrastructure: Proceedings of a Workshop*. The National Academies Press. https://doi.org/10.17226/26128

National Academies of Sciences, Engineering, and Medicine. (2022). *Planning the Future Space Weather Operations and Research Infrastructure: Proceedings of the Phase II Workshop*. The National Academies Press. https://doi.org/10.17226/26712

Pavón-Carrasco, F. J., & De Santis, A. (2016). The South Atlantic anomaly: The key for a possible geomagnetic reversal. *Frontiers in Earth Science*, *4*, 40. https://doi.org/10.3389/feart.2016.00040

Qin, M., Zhang, X., Ni, B., Song, H., Zou, H., & Sun, Y. (2014). Solar cycle variations of trapped proton flux in the inner radiation belt. *Journal of Geophysical Research: Space Physics*, *119*(12), 9658–9669. https://doi.org/10.1002/2014JA020300

Schulz, M., & Lanzerotti, L. J. (1974). Particle diffusion in the radiation belts. In *Particle diffusion in the radiation belts. Series: Physics and chemistry in space*. https://doi.org/10.1007/978-3-642-65675-0

Selesnick, R. S., & Albert, J. M. (2019). Variability of the proton radiation belt. *Journal of Geophysical Research: Space Physics*, *124*(7), 5516–5527. https://doi.org/10.1029/2019JA026754

Selesnick, R. S., Looper, M. D., & Mewaldt, R. A. (2007). A theoretical model of the inner proton radiation belt. *Space Weather*, *5*(4), S04003. https://doi.org/10.1029/2006SW000275

Stassinopoulos, E. G., & Raymond, J. P. (1988). The space radiation environment for electronics. *Proceedings of the IEEE*, *76*(11), 1423–1442. https://doi.org/10.1109/5.90113

Svalgaard, L., Cliver, E. W., & Kamide, Y. (2005). Sunspot cycle 24: Smallest cycle in 100 years? *Geophysical Research Letters*, *32*(1), L01104. https://doi.org/10.1029/2004GL021664

Upton, L. A., & Hathaway, D. H. (2018). An updated solar cycle 25 prediction with AFT: The modern minimum. *Geophysical Research Letters*, *45*(16), 8091–8095. https://doi.org/10.1029/2018GL078387

Upton, L. A., & Hathaway, D. H. (2023). Solar cycle precursors and the outlook for cycle 25. *Journal of Geophysical Research: Space Physics*, *128*(10), e2023JA031681. https://doi.org/10.1029/2023JA031681

Yue, J., & Wang, W. (2024). Thermosphere. In G. R. North, J. Pyle, & F. Zhang (Eds.), *Encyclopedia of Atmospheric Sciences* (2nd ed., pp. 402–408). Academic Press. (Note: This is an update to the previous edition article by S. C. Solomon and R. G. Roble, 2015). https://doi.org/10.1016/B978-0-12-382225-3.00408-4